Adaptive algorithms for the rejection of sinusoidal disturbances acting on unknown plants

Scott Pigg, *Grad. Student Member, IEEE,* and Marc Bodson, *Fellow, IEEE*

Abstract

The rejection of periodic disturbances is a problem frequently encountered in control engineering, and in active noise and vibration control in particular. The paper presents a new adaptive algorithm for situations where the plant is unknown and may be time-varying. The approach consists in obtaining on-line estimates of the plant frequency response and of the disturbance parameters. The estimates are used to continuously update control parameters and cancel or minimize the effect of the disturbance. The dynamic behavior of the algorithm is analyzed using averaging theory. Averaging theory is used to approximate the nonlinear time-varying closed-loop system by a nonlinear time-invariant system. It is shown that the four-dimensional averaged system has a two-dimensional equilibrium surface, which can be divided into stable and unstable subsets. Trajectories generally converge to a stable point of the equilibrium surface, implying that the disturbance is asymptotically cancelled even if the true parameters of the system are not exactly determined. Simulations, as well as extensive experiments on an active noise control testbed, illustrate the results of the analysis, and demonstrate the ability of the algorithm to recover from abrupt system changes or track slowly-varying parameters. Extensions of the algorithm to systems with multiple inputs/outputs and disturbances consisting of multiple frequency components are provided.

I. Introduction

The paper considers the rejection of unknown disturbances, with a particular interest in active noise and vibration control applications *(*ANC, AVC, or ANVC) and on disturbances that are the sum of periodic signals. Examples of applications include active control of noise in turboprop aircraft [33], vibration reduction in helicopters [24] [5], reduction of optical jitter in laser communication systems [17], isolation in space structures of vibrations produced by control moment gyroscopes and cryogenic coolers [14] [15], regulation of tension in paper machines [37] and in continuous steel casting processes [31], limitation of periodic shaft deviations in magnetic bearing systems [4],

Manuscript received January 15, 2008. This material is based upon work supported in part by the National Science Foundation under Grant No. ECS0115070 and in part by Sandia National Laboratories.

S. Pigg and M. Bodson are with the Department of Electrical and Computer Engineering, University of Utah, 50 S Central Campus Dr Rm 3280, Salt Lake City, UT 84112, U.S.A. (email: scott.pigg@utah.edu; bodson@eng.utah.edu).

S. Pigg is available for correspondence and return of proofs.

track following despite eccentricity in disk drives [1] [25] and CD players [11] [20], and suppression of gearbox housing vibrations [36].

The paper proposes a new algorithm for the rejection of sinusoidal disturbances of known frequency acting on systems with dynamics that are unknown and may vary in unpredictable ways. An example is the active control of noise, where the dynamics of sound transmission can be considerably affected by people moving within the space where sound propagates. The algorithm of the paper enables engineers to tackle such a difficult problem for which few practical solutions exist. Indeed, while a limited set of solutions have been proposed, an even smaller subset has been proved to work in practice or has been analyzed carefully.

In the signal processing literature, algorithms have been presented that combine a gradient algorithm (*i.e.,* adaptive least-mean-squares or LMS algorithm) with an on-line identifier of the plant's impulse response [27][21][22]. Such methods require considerable excitation to be injected in the form of white noise added at the input of the system for the identification. An analysis of the stability of the closed-loop system is also not provided in the papers, let alone any insight into the dynamics of the systems.

Adaptive control theory provides an option for the control of unknown systems with unknown periodic disturbances. The idea, as proposed in [8], [9] [16], is to apply the internal model principle within a model reference or pole placement adaptive control strategy. Practically, the implementation is obtained by raising the order of the controller and forcing some poles of the controller on the unit circle (or the $j\omega$-axis in continuous-time). Global stability of such systems can be proved in theory, even allowing for unstable plants and for tracking of arbitrary reference inputs. Unfortunately, there is evidence of slow convergence and poor robustness properties of these schemes in the literature [38] [19]. It is possible that the robustness problems could be reduced or resolved using robust adaptive control methods [10], [23]. However, we are not aware of any report of the practical viability of these methods in disturbance rejection applications. Further, additional problems make it difficult to apply the methods to the type of problems being considered:

- the number of adaptive parameters is two times the order of the plant plus two times the number of sinusoidal components. Considering that an appropriate model for an active noise control system is a finite impulse response (FIR) system with 200 parameters or so, the adaptive controller is of very high order, and identification of the parameters is difficult.
- model reference and pole placement methods assume a known plant delay. In ANC, this delay is not known *a priori*, and may vary.

Harmonic steady-state (HSS) methods have simplified the problem by approximating the plant by its steady-state sinusoidal response. In [5], Pratt and co-workers described an HSS algorithm known as higher harmonic control (HHC), for use in the reduction of vibrations in helicopters. In [13], the algorithm was used for the cancellation of periodic noise in an acoustic drum. A proof of stability was provided in [13], although the authors assumed the injection of an excitation signal to ensure correct identification of the plant. In contrast, [32] proposed a clever algorithm that combined two gradient-type adaptation steps to obtain an algorithm with guaranteed stability properties and without additional excitation. The proof is based on a small gain argument that requires an upper

bound on the plant's frequency response and a sufficiently small adaptation gain. While successful experiments were reported in [32], no data was shown on the transient properties of the algorithm or on its ability to track variations in the parameters.

The main contributions of this paper are:

- a remarkably simple adaptive HSS algorithm that eliminates the need for batches of data as in [13] (control parameters are updated continuously).
- a verification of the performance of the algorithm through active noise control experiments, demonstrating the ability to track abruptly or continuously time-varying system parameters in a challenging, practical application.
- a stability analysis based on the theory of averaging that does not require the addition of external excitation signals and provides useful insight in the dynamics of the adaptive system.

Note that rigorous stability proofs have been the subject of much research in adaptive control, but often turn out to be very complicated and to provide no insight about the dynamics of the systems. As an alternative, averaging methods have provided approximate results that are far more useful [3] [30] [12]. Averaging theory shows how a set of nonlinear time-varying differential equations can be approximated by a much simpler averaged system. In [30] and other work, averaging theory was found to provide invaluable information on the dynamic properties of specific adaptive control systems. For periodic disturbance rejection problems, averaging theory is even more powerful, because the conditions for the existence of the averaged system are generally satisfied without additional assumptions, due to the periodic nature of the signals. While averaging theory requires low adaptation gains, experience shows that the approximation is useful for the typical adaptation gains used in practice, and that the loss of rigor due to the approximation is more than compensated for by the powerful insights that the approximation provides.

The paper is organized as follows. After formulating the system's equations using a gradient–based identifier, averaging theory [30] is reviewed. The averaged system associated with the problem is found and simulations are used to demonstrate the closeness of the responses. Next, the equilibrium points of the averaged system are determined and an eigenanalysis is used to understand the system's behavior around the equilibrium. This analysis enables one to understand how the algorithm handles uncertainty in the plant parameters in a way that a standard adaptive algorithm without plant adaptation is unable to. Further simulations illustrate the results of the analysis of the averaged system, and active noise control experiments validate the analysis further. Experimental results using a standard LMS algorithm are presented for comparison. Finally, experiments are reported using a *least-squares* identifier and demonstrate the ability of the algorithm to track time-varying parameters. For clarity we confine our presentation to a single-input single-output plant and a single tone disturbance; however, extensions of the algorithm to multi-input multi-output plants and multi-tone disturbances are provided.

II. Adaptive algorithm

A. System formulation

Consider the feedback system shown in Fig. 1. The output of the plant

$$y(t) = P(s)[u(t)] + p(t) \tag{1}$$

is fed back in order to determine the control signal $u(t)$ needed to reject the sinusoidal disturbance $p(t)$. The notation $P(s)[(\cdot)]$ represents the time-domain output of the system with transfer function $P(s)$. $P(s)$ is assumed to be a bounded input-bounded-output stable linear time-invariant system, but is otherwise unknown. Although the plant is fixed in the analysis, experiments show that the use of adaptation allows the plant to vary significantly over time. The compensator C is generally a nonlinear and time-varying control law consisting of a parameter identification scheme and a disturbance cancellation algorithm.

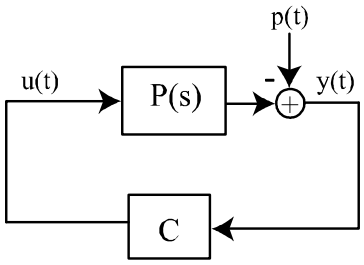

Fig. 1. Feedback control system.

The disturbance is assumed to be a sinusoidal signal given by

$$p(t) = p_c \cos(\omega_1 t) + p_s \sin(\omega_1 t) = w_1^T(t)\pi^* \tag{2}$$

where

$$\pi^* = \begin{pmatrix} p_c \\ p_s \end{pmatrix}, \quad w_1 = \begin{pmatrix} \cos(\omega_1 t) \\ \sin(\omega_1 t) \end{pmatrix} \tag{3}$$

and ω_1 is the known frequency of the disturbance signal. Under these conditions, a control signal of the form

$$u(t) = \theta_c \cos(\omega_1 t) + \theta_s \sin(\omega_1 t) = w_1^T(t)\theta \tag{4}$$

is sufficient to cancel the disturbance in steady-state, provided that the controller parameter vector

$$\theta = \begin{pmatrix} \theta_c \\ \theta_s \end{pmatrix} \tag{5}$$

is chosen appropriately.

B. Adaptive harmonic steady-state algorithm

For the derivation of the algorithm, the response of the plant is approximated by the sinusoidal steady-state response [5]

$$y(t) \simeq y_{ss}(t) = w_1^T(t) G^* \theta + p(t) = w_1^T(t) \left(G^* \theta + \pi^* \right) \tag{6}$$

where

$$G^* = \begin{pmatrix} P_R & P_I \\ -P_I & P_R \end{pmatrix} \tag{7}$$

and P_R, P_I are the real and imaginary parts of the plant's frequency response evaluated at ω_1

$$P(j\omega_1) \triangleq P_R + jP_I \tag{8}$$

Although the expression may not look familiar to the reader, the result is a straightforward application of the general formula for the steady-state sinusoidal response of a linear time-invariant system [7, p. 459].

In the problem considered here, there are four unknowns: two are associated with the plant (P_R and P_I) and two are associated with the disturbance (p_c and p_s). The parameters, whose estimate will be part of the internal state of the controller, are collected in a vector

$$x^* = \begin{pmatrix} P_R & P_I & p_c & p_s \end{pmatrix}^T \tag{9}$$

so that the steady-state output of the plant (6) can be written as

$$y_{ss}(t) = W^T(t, \theta) x^* \tag{10}$$

where $W(t, \theta)$ is a so-called *regressor matrix*

$$W(t, \theta) = \begin{pmatrix} \theta_c \cos(\omega_1 t) + \theta_s \sin(\omega_1 t) \\ \theta_s \cos(\omega_1 t) - \theta_c \sin(\omega_1 t) \\ \cos(\omega_1 t) \\ \sin(\omega_1 t) \end{pmatrix}. \tag{11}$$

On the basis of the linear expression in (10), an estimate x of the unknown parameter vector x^* can be obtained using a gradient or a least-squares algorithm [30, p. 57]. For example, a gradient algorithm for the minimization of the squared error $e^2 = \left(W^T x - y \right)^2$ that uses the approximation $y(t) \simeq y_{ss}(t)$ is given by

$$\dot{x}(t) = -\epsilon W(t, \theta) \left(W^T(t, \theta) x(t) - y(t) \right) \tag{12}$$

The parameter $\epsilon > 0$ is the adaptation gain, which will be assumed to be small in the application of the averaging theory later in the paper.

Having derived an algorithm for the estimation of the unknown parameters, it remains to define the control law. Note that, from (6), the disturbance is known to be cancelled exactly in steady-state for a nominal control parameter

$$\theta^* = -G^{*-1} \pi^* \tag{13}$$

Given an estimate of the unknown parameter vector x, a certainty equivalence control law [30, p. 268] will redefine θ as $\theta(x)$, a function of the estimate x, using

$$G(x) = \begin{pmatrix} x_1 & x_2 \\ -x_2 & x_1 \end{pmatrix}, \ \pi(x) = \begin{pmatrix} x_3 \\ x_4 \end{pmatrix} \tag{14}$$

and

$$\begin{aligned} \theta(x) &= \begin{pmatrix} \theta_c(x) \\ \theta_s(x) \end{pmatrix} = -G^{-1}(x)\pi(x) \\ &= -\frac{1}{x_1^2 + x_2^2} \begin{pmatrix} x_1x_3 - x_2x_4 \\ x_1x_4 + x_2x_3 \end{pmatrix} \end{aligned} \tag{15}$$

The nominal values satisfy

$$G^* = G(x^*), \ \pi^* = \pi(x^*), \text{ and } \theta^* = \theta(x^*) \tag{16}$$

A state-space representation of the overall system can be obtained as follows. With x_P denoting the states of $P(s) = C(sI - A)^{-1}B$, the plant has the following state-space representation

$$\begin{aligned} \dot{x}_P(t) &= Ax_P(t) + Bu(t) \\ &= Ax_P(t) + Bw_1^T(t)\theta(x) \end{aligned} \tag{17}$$

$$y(t) = Cx_P(t) + p(t) = Cx_P(t) + w_1^T(t)\pi^* \tag{18}$$

Defining

$$E(x) = \begin{pmatrix} D(x) \\ I_{2\times 2} \end{pmatrix}, \ D(x) = \begin{pmatrix} \theta_c(x) & \theta_s(x) \\ \theta_s(x) & -\theta_c(x) \end{pmatrix} \tag{19}$$

the matrix $W(t, \theta)$ is given by

$$W(t, \theta) = E(x)w_1^T(t). \tag{20}$$

Then, the overall system is described by a set of differential equations with two vectors x and x_P composing the total state vector and

$$\dot{x}_P = Ax_P + Bw_1^T(t)\theta(x) \tag{21}$$

$$\dot{x} = -\epsilon E(x)w_1(t)\left(w_1^T(t)E^T(x)x - Cx_P - w_1^T(t)\pi^*\right) \tag{22}$$

with (15), (19) giving the functions $\theta(x)$ and $E(x)$. Note that this set of differential equations is both time-varying and nonlinear, making direct analysis difficult. Fortunately, under the assumption of small gain ϵ, the application of averaging theory produces an approximate nonlinear time-invariant system whose dynamics can be analyzed and provide interesting insights in the behavior of the system.

C. Alternative solution

In the formulation presented in this paper, the algorithm has the structure of Fig. 2, where

$$\begin{aligned} \tilde{u}(t) &= \tilde{w}_1^T(t)\theta \\ \tilde{w}_1(t) &= \begin{pmatrix} -\sin(\omega_1 t) \\ \cos(\omega_1 t) \end{pmatrix}. \end{aligned} \tag{23}$$

In [28], a different implementation of the same concept was proposed, whereby the regressor variables would vary at a slower rate. The vector y_a was defined as

$$y_a = \begin{pmatrix} y_c \\ y_s \end{pmatrix} = AVG\left[2w_1(t)y(t)\right] = G^*\theta + \pi^*. \tag{24}$$

where the averaging operation AVG could be performed by averaging the signals over some multiple of the period T of the signals. Using this approach, the system was parameterized in terms of the regressor

$$W(t) = \begin{pmatrix} \theta_c(t) & \theta_s(t) & 1 & 0 \\ \theta_s(t) & -\theta_c(t) & 0 & 1 \end{pmatrix}^T \tag{25}$$

which corresponds to the system of Fig. 3. In this formulation, the regressor signals (25) vary at a slower rate as compared to (11), which varies with the periodic fluctuation of $w_1(t)$. Both approaches have been tested in experiments, with comparable results. In the implementation of [28], the averaging operation was simply neglected, on the basis that slow adaptation would provide the necessary smoothing. Here we use a similar argument for the analysis of the adaptive system, relying on a more formal application of averaging theory.

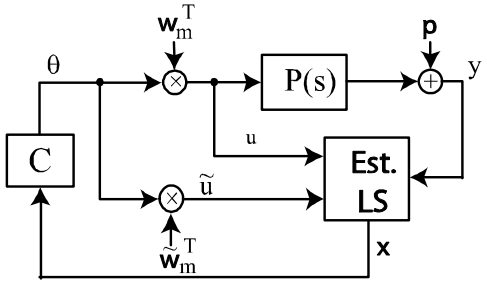

Fig. 2. Proposed control system.

III. Averaging analysis

A. Background - mixed time scale systems

Of particular interest to our problem is the continuous-time averaging method for mixed time scale systems as discussed in [30, p.186]. The theory applies to systems of the form

$$\dot{x} = \epsilon f(t, x, x_P) \tag{26}$$

$$\dot{x}_P = Ax_P + h(t, x) \tag{27}$$

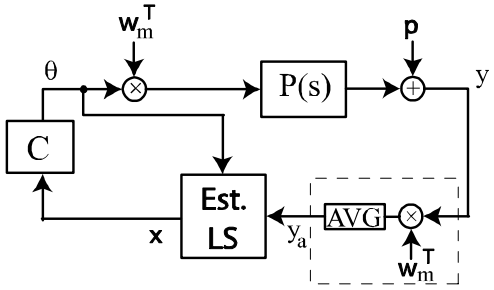

Fig. 3. Alternative control system.

which includes the problem under consideration if one defines

$$f(t,x,x_P) = -E(x)w_1(t)\left(w_1^T(t)E^T(x)x - Cx_P - w_1^T(t)\pi^*\right) \quad (28)$$

$$h(t,x) = Bw_1^T(t)\theta(x) \quad (29)$$

For ϵ small, x is a slow variable, while x_P varies faster, except through its dependency on x. Averaging theory shows how the trajectories of (26)-(27) can be related to the trajectories of the so-called averaged system

$$\dot{x} = \epsilon f_{av}(x) \quad (30)$$

where

$$f_{av}(x) = \lim_{T\to\infty}\frac{1}{T}\int_{t_0}^{t_0+T} f(\tau,x,v(\tau,x))d\tau \quad (31)$$

and

$$v(t,x) := \int_0^t e^{A(t-\tau)}h(\tau,x)d\tau. \quad (32)$$

Central to the method of averaging is the assumption that the limit in (31) exist uniformly in t_0 and x. In other words, there exists a strictly decreasing continuous function $\gamma(T)$, such that $\gamma(T)\to 0$ as $T\to\infty$ and

$$\left|\frac{1}{T}\int_{t_0}^{t_0+T} f(\tau,x,v(\tau,x))d\tau - f_{av}(x)\right| \le \gamma(T). \quad (33)$$

The function $\gamma(T)$ is called the convergence function. If the limit exists, ϵ is sufficiently small, and certain technical conditions are satisfied, the response of (26)-(27) is close to the response of (30). Specifically, the theory is based on the following assumptions.

Assumptions

Given some arbitrary vector $x\in R^n$ and for some $h>0$ such that $B_h = \{x\in\mathbb{R}^n \,|\, \|x\| < h\}$

B1 The function f is a piecewise continuous function of time, and a continuous function of x and x_P. Moreover, for some l_1, $l_2 \ge 0$

$$|f(t,x_a,x_{P,a}) - f(t,x_b,x_{P,b})| \le l_1|x_a - x_b| + l_2|x_{P,a} - x_{P,b}|$$

for all $t \geq 0$, x_a, $x_b \in B_h$, $x_{P,a}$, $x_{P,b} \in B_h$. Also assume that $f(t, x, v(t, x))$ has continuous and bounded first partial derivatives with respect to x for all $t \geq 0$ and $x \in B_h$.

B2 The function $f(t, x, v(t, x))$ has average value $f_{av}(x)$. Moreover, $f_{av}(x)$ has continuous and bounded first partial derivatives with respect to x, for all $x \in B_h$, so that for some $l_{av} \geq 0$

$$|f_{av}(x_a) - f_{av}(x_b)| \leq l_{av} |x_a - x_b|$$

for all x_a, $x_b \in B_h$.

B3 Let $d(t, x) = f(t, x, v(t, x)) - f_{av}(x)$, so that $d(t, x)$ has zero average value. Assume that the convergence function can be written as $\gamma(T) |x| + \tilde{\gamma}(T)$, where $\tilde{\gamma}(T)$ decays exponentially to zero. Additionally, $\frac{\partial d(t,x)}{\partial x}$ has zero average value, with convergence function $\gamma(T)$.

The following result can then be obtained [30, p.184]:

*Lemma 1 (**Perturbation Formulation of Averaging**):* If the mixed time scale system (26)-(27) and the averaged system (30) satisfy assumptions B1-B4. Then, there exists a bounded function $w_\epsilon(t, x)$, whose first partial derivative with respect to time is arbitrarily close to $d(t, x)$ and a class K function $\xi(\epsilon)$ such that the transformation

$$x = z + \epsilon w_\epsilon(t, x) \tag{34}$$

is a homeomorphism in B_h for all $\epsilon \leq \epsilon_1$, where $\epsilon_1 > 0$. Under the transformation, system (26) becomes

$$\dot{z} = \epsilon f_{av}(z) + \epsilon p_1(t, z, \epsilon) + \epsilon p_2(t, z, x_P, \epsilon) \tag{35}$$

$$z(0) = x(0) \tag{36}$$

where

$$|p_1(t, z, \epsilon)| \leq \xi(\epsilon) k_1 |z| \tag{37}$$

$$|p_2(t, z, x_P, \epsilon)| \leq k_2 |x_{P,zi}| \tag{38}$$

for some k_1, k_2 depending on l_1, l_2, l_{av}.

A proof of *Lemma 1* can be found in [30, p.348]. This proof establishes a link between the convergence function $\gamma(T)$ and the order of the bound in (37). In particular, if $d(t, x)$ in assumption B3 has a bounded integral with respect to time, then $\gamma(T) \sim \frac{1}{T}$ and it can be shown that $\xi(\epsilon)$ is on the order of ϵ. The bound in (38) is determined by the convergence properties of $x_{P,zi} = x_P - v(t, x)$, which is the zero-input response of x_P.

Lemma 1 is fundamental to the theory of averaging. It allows a system satisfying certain conditions to be written as a perturbation of the averaged system and it shows that the perturbation terms are bounded. By imposing further restrictions, conclusions can then be drawn concerning the closeness of the original and averaged systems. Consider the additional assumptions:

B4 A is exponentially stable.

B5 Let $x_{av}(t)$ specify the solution of the averaged system (30). For some $h' < h$, $|x_{av}(t)| \in B_{h'}$ on the time intervals considered, and for some h_0, $x_P \in B_{h_0}$.

B6 $h(t,0) = 0$ for all $t \geq 0$, and $\left\| \frac{\partial h(t,x)}{\partial x} \right\|$ is bounded for all $t \geq 0$, $x \in B_h$.

Then, the following result can be obtained.

*Lemma 2 (**Basic Averaging Lemma**):* If the mixed time scale system (26)-(27) and the averaged system (30) satisfy assumptions B1-B6, then there is an ϵ_T, $0 < \epsilon_T \leq \epsilon_0$ and a class K function $\Psi(\epsilon)$ such that

$$\|x(t) - x_{av}(t)\| \leq \Psi(\epsilon) b_T \tag{39}$$

for some $b_T > 0$ and for all $t \in [0, T/\epsilon]$ and $0 < \epsilon \leq \epsilon_T$. Further, $\Psi(\epsilon)$ is on the order of $\xi(\epsilon) + \epsilon$.

A proof of *Lemma 2* can be found in [30, p.349]. *Lemma 2* states that, for ϵ sufficiently small, the trajectories of (26) and (30) can be made arbitrarily close for all $t \in [0, T/\epsilon]$. This allows insight into the behavior of (26)-(27) by studying the behavior of (30). Also, when $d(t,x)$ in assumption B3 has a bounded integral with respect to time, $\Psi(\epsilon)$ is on the order of ϵ. This condition is satisfied for the system under consideration due to the sinusoidal nature of the signals.

B. Averaged system

We found earlier that the system under consideration fitted the averaging framework. It remains to determine what the averaged system is, whether the assumptions are satisfied, and what interesting properties the averaged system may have. The parameter vector x is frozen in the computation of the averaged system [30, p.162]. Further, all of the time variation in the functions is due to sinusoidal signals, and the systems to which they are applied are linear time-invariant systems. The outcome is that the average of the function $f(t, x, x_P)$ is well-defined and can be computed exactly. Specifically, the function

$$\begin{aligned} v(t,x) &= \int_0^t e^{A(t-\tau)} B w_1(\tau) d\tau \cdot \theta(x) && (40) \\ &= x_{P,ss}(t) + x_{P,tr}(t) && (41) \end{aligned}$$

where $x_{P,ss}(t)$ is the steady-state response of the state of the plant to the sinusoidal excitation $w_1(t)$ and, $x_{P,tr}$ is a transient response that decays to 0 exponentially, given that A is exponentially stable.

The averaged system is obtained by computing the average of

$$f_{av}(x) = -\lim_{T \to \infty} \frac{1}{T} \int_{t_0}^{t_0+T} E(x) w_1(\tau) \left(w_1^T(\tau) E^T(x) x - C v(\tau, x) - w_1^T(\tau) \pi^* \right) d\tau \tag{42}$$

where

$$\begin{aligned} C v(t,x) + w_1^T(t)\pi^* &= C x_{P,ss}(t) + C x_{P,tr}(t) + w_1^T(t)\pi^* \\ &= y_{ss}(t) + y_{tr}(t) && (43) \end{aligned}$$

and $y_{tr}(t) = C x_{P,tr}(t)$. Equations (10) and (20) imply that

$$y_{ss}(t) = w_1^T(t) E^T(x) x^* \tag{44}$$

and since the transient response of the plant does not affect the average value of the function,

$$f_{av}(x) = -\lim_{T\to\infty}\frac{1}{T}\int_{t_0}^{t_0+T} E(x)w_1(\tau)\left(w_1^T(\tau)E^T(x)x - w_1^T(\tau)E^T(x)x^*\right)d\tau \tag{45}$$

$$= -E(x)\left(\lim_{T\to\infty}\frac{1}{T}\int_{t_0}^{t_0+T} w_1(\tau)w_1^T(\tau)d\tau\right)E^T(x)(x-x^*) \tag{46}$$

$$= -\frac{1}{2}E(x)E^T(x)(x-x^*) \tag{47}$$

In other words, the averaged system is simply given by

$$\dot{x} = -\frac{\epsilon}{2}\begin{pmatrix} D(x) \\ I_{2\times 2}\end{pmatrix}\begin{pmatrix} D(x) & I_{2\times 2}\end{pmatrix}(x-x^*) \tag{48}$$

with (15) and (19) giving

$$D(x) = \frac{1}{x_1^2+x_2^2}\begin{pmatrix} x_1x_3 - x_2x_4 & x_1x_4 + x_2x_3 \\ x_1x_4 + x_2x_3 & -x_1x_3 + x_2x_4\end{pmatrix} \tag{49}$$

Although (48)-(49) describe a nonlinear system, the method of averaging has eliminated the time variation of the original system, providing an opportunity to understand much better the dynamics of the system.

C. Application of Averaging Theory

The application of the theory is relatively straightforward, and verification of the assumptions is left to the appendix. A technical difficulty is related to the fact that both the adaptive and the averaged systems have a singularity at $x_1^2 + x_2^2 = 0$ (see equations (15) and (49)). Such singularities are quite common in adaptive control, occurring any time the estimate of the gain of the plant is zero. Here, the singularity occurs when the estimate of the plant's frequency response is zero, a problem that is somewhat unlikely to occur as *two* parameters need to be small for the singularity to be reached. Nevertheless, a cautious implementation of the algorithm would apply one of the available techniques to address singularities. For example, a simple practical fix consists in using in the control law either the parameter x if $x_1^2 + x_2^2 \geqslant \delta > 0$, where δ is a small parameter, or else the last value of the estimated parameter x that satisfied the condition. As far as the theory is concerned, we avoid the difficulty by adding the following assumption:

B7 Assume that trajectories of the original and averaged system are such that $x_1^2 + x_2^2 \geqslant \delta$ for some $\delta > 0$.

Using assumptions B1-B7, it is verified in appendix that the system given by (12)-(17) satisfies the conditions of the theory. Thus, *Lemma 1* and *Lemma 2* can be applied. In the verification of assumption B3, one finds that $d(t,x)$ has a bounded integral with respect to time, suggesting that $\xi(\epsilon)$ in *Lemma 1* is of the order of ϵ. *Lemma 2* establishes that (48) can be used as an order of ϵ approximation of (12)-(17) for all $t \in [0, T/\epsilon]$. Note that *Lemma 2* only shows closeness of the original and averaged systems over finite time. Any stability properties connecting the original and the averaged system would require a different theorem. The theorems of [30] do not apply because they assume a unique equilibrium point of the averaged system. As we will see, this is not the case here.

D. Simulation example

To show the closeness of the responses (12)-(17) and (48), we let $\omega_1 = 330\pi$ and the plant is taken as a 250 coefficient FIR transfer function. The transfer function was measured from an active noise control system using a white noise input and a gradient search identification procedure. The initial parameter estimate was $x(0) = x_{av}(0) = \begin{pmatrix} 1.0 & 1.0 & 0 & 0 \end{pmatrix}^T$. In Fig. 4, the response of the first adaptive parameter x_1 is shown. Four responses are shown: the averaged system with $\epsilon = 1$ (solid line), the actual system for $\epsilon = 100$ (dashed dot), the actual system for $\epsilon = 50$ (dashed), and the actual system for $\epsilon = 1$ (circles). As ϵ decreases, one finds that the trajectory of the original system approaches that of the averaged system. Note that the parameter estimates do not converge to the nominal values, indicating that the regressor (11) is not persistently exciting [30, p.73]. However, the control parameters θ_c and θ_s do converge to the nominal values, resulting in cancellation of the disturbance for all values of ϵ. The control parameters are shown in Fig. 5, along with θ^*, the nominal value that exactly cancels the disturbance (the constant line).

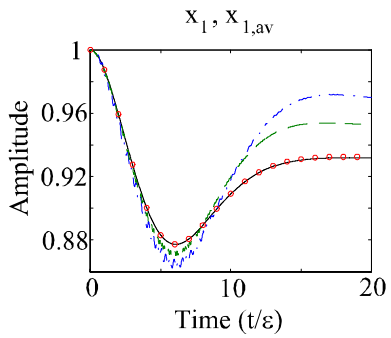

Fig. 4. The response of the first adapted parameter x_1 for the averaged system and three responses of the actual system.

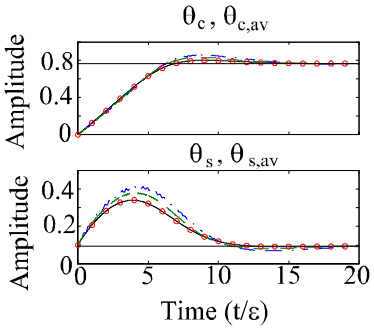

Fig. 5. Trajectories of control parameters for the actual and the averaged systems.

IV. Properties of the averaged system

Several properties of the averaged system can be derived from the rather simple form that was obtained in (48)-(49), enabling one to gain insight on the behavior of the closed-loop system.

A. Equilibrium surface

From the expression of the averaged system (48), we deduce that an equilibrium point of the averaged system must satisfy

$$E^T(x)(x-x^*) = \begin{pmatrix} D(x) & I_{2\times 2} \end{pmatrix}(x-x^*) = 0 \tag{50}$$

Therefore, $x = x^*$ is an equilibrium point of the system. It is not the only one, however. Using (14)-(15)

$$\begin{aligned} \begin{pmatrix} D(x) & I_{2\times 2} \end{pmatrix} x &= \begin{pmatrix} \theta_c(x) & \theta_s(x) \\ \theta_s(x) & -\theta_c(x) \end{pmatrix} \begin{pmatrix} x_1 \\ x_2 \end{pmatrix} + \begin{pmatrix} x_3 \\ x_4 \end{pmatrix} && (51) \\ &= \begin{pmatrix} x_1 & x_2 \\ -x_2 & x_1 \end{pmatrix} \begin{pmatrix} \theta_c(x) \\ \theta_s(x) \end{pmatrix} + \begin{pmatrix} x_3 \\ x_4 \end{pmatrix} && (52) \\ &= 0 && (53) \end{aligned}$$

In other words, $E^T(x)x = 0$ and equilibrium points must satisfy

$$E^T(x)x^* = 0 \tag{54}$$

(54) can be rewritten as

$$\begin{aligned} \begin{pmatrix} \theta_c(x) & \theta_s(x) \\ \theta_s(x) & -\theta_c(x) \end{pmatrix} \begin{pmatrix} x_1^* \\ x_2^* \end{pmatrix} + \begin{pmatrix} x_3^* \\ x_4^* \end{pmatrix} &= \begin{pmatrix} x_1^* & x_2^* \\ -x_2^* & x_1^* \end{pmatrix} \begin{pmatrix} \theta_c(x) \\ \theta_s(x) \end{pmatrix} + \begin{pmatrix} x_3^* \\ x_4^* \end{pmatrix} \\ &= 0 && (55) \end{aligned}$$

or

$$\begin{aligned} \begin{pmatrix} \theta_c(x) \\ \theta_s(x) \end{pmatrix} &= -\begin{pmatrix} x_1^* & x_2^* \\ -x_2^* & x_1^* \end{pmatrix}^{-1} \begin{pmatrix} x_3^* \\ x_4^* \end{pmatrix} && (56) \\ &= \begin{pmatrix} \theta_c^* \\ \theta_s^* \end{pmatrix} && (57) \end{aligned}$$

The last equation shows that any equilibrium state results in the cancellation of the disturbance, confirming the observation made in section III D. Equation (57) also implies, with (14)-(15), that

$$\begin{pmatrix} x_1 & x_2 \\ -x_2 & x_1 \end{pmatrix}^{-1} \begin{pmatrix} x_3 \\ x_4 \end{pmatrix} = -\begin{pmatrix} \theta_c^* \\ \theta_s^* \end{pmatrix} \tag{58}$$

or, reorganizing the terms,

$$\begin{pmatrix} x_3 \\ x_4 \end{pmatrix} = -\begin{pmatrix} \theta_c^* & \theta_s^* \\ \theta_s^* & -\theta_c^* \end{pmatrix} \begin{pmatrix} x_1 \\ x_2 \end{pmatrix} \tag{59}$$

In other words, the set of equilibrium points is a two-dimensional linear subspace of the four-dimensional state-space. The set includes the nominal parameter x^*. Note that, for x constant,

$$f(t, x, x_{P,ss}) = -E(x)w_1(t)w_1^T(t)E^T(x)(x - x^*). \tag{60}$$

Therefore, any equilibrium state of the averaged system is also an equilibrium state of the original system. This result further explains why, in section III.D., all the trajectories were such that θ converged to θ^*. Further, (44) indicates that any equilibrium state corresponds to a perfect rejection of the disturbance.

B. Local stability

The local stability of the averaged system can be determined by linearizing (48) around an equilibrium state x. The following eigenvalues were computed using the Maple kernel

$$\lambda = \begin{pmatrix} 0 \\ 0 \\ \left(\frac{x_2^* + jx_1^*}{x_2 + jx_1}\right)\beta \\ \left(\frac{x_2^* - jx_1^*}{x_2 - jx_1}\right)\beta \end{pmatrix} \tag{61}$$

where $\beta = -\frac{\epsilon}{2}\left(\frac{x_1^{*2}+x_2^{*2}+x_3^{*2}+x_4^{*2}}{x_1^{*2}+x_2^{*2}}\right)$. The two eigenvalues at zero confirm the two-dimensional nature of the linear equilibrium surface. The nonzero eigenvalues are complex conjugates that lie in the open left-half plane if and only if

$$x_1 x_1^* + x_2 x_2^* > 0 \tag{62}$$

or equivalently

$$x_3 x_3^* + x_4 x_4^* > 0. \tag{63}$$

For the reverse signs, the eigenvalues lie in the open right half plane. The stability condition can be interpreted in the (x_1, x_2) plane, as shown in Fig. 6. Specifically, the line going through the origin that is perpendicular to the line joining (0, 0) and (x_1^*, x_2^*) defines the boundary between the stable and unstable states. Interestingly, this is the same boundary that delineates the stable and unstable regions of a standard LMS algorithm that does not identify the plant parameters [6], as will be discussed in section V.B. In this case, however, the nonlinear dynamics ensure that all trajectories eventually converge to the stable subset of the equilibrium surface.

C. Lyapunov analysis

Lyapunov arguments can be used to establish further stability results for the averaged system. Specifically, the Lyapunov candidate function

$$V = \|x(t) - x^*\|^2 \tag{64}$$

evaluated along the trajectories of (48) gives

$$\dot{V} = -\epsilon \left\| E^T(x)\,(x - x^*) \right\|^2 \leq 0 \tag{65}$$

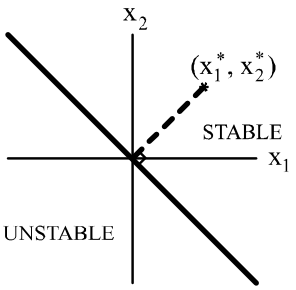

Fig. 6. Relationship between the location on the equillibrium surface and stability

which implies that

$$\|x(t) - x^*\| \leq \|x(0) - x^*\| \tag{66}$$

for all $t > 0$. Since x and $\dot{x}$ are bounded (using (48) and assumption B7), one may also deduce that $E^T(x)\,(x - x^*) \rightarrow 0$ as $t \rightarrow \infty$. In turn, $E^T(x)x = 0$ and (44) imply that the disturbance is asymptotically cancelled.

Further results may be obtained by noting that

$$\left(\begin{array}{cc} -I_{2\times 2} & D(x) \end{array} \right) E(x) = 0 \tag{67}$$

so that

$$\left(\begin{array}{cc} -I_{2\times 2} & D(x) \end{array} \right) \dot{x} = 0 \tag{68}$$

Using (14)-(15)

$$D(x) = \left(\begin{array}{cc} \theta_c(x) & \theta_s(x) \\ \theta_s(x) & -\theta_c(x) \end{array} \right) \tag{69}$$

$$= -\left(\begin{array}{cc} x_1 & x_2 \\ -x_2 & x_1 \end{array} \right)^{-1} \left(\begin{array}{cc} x_3 & x_4 \\ x_4 & -x_3 \end{array} \right) \tag{70}$$

The result implies that

$$\left(\begin{array}{cccc} x_1 & x_2 & x_3 & x_4 \\ -x_2 & x_1 & x_4 & -x_3 \end{array} \right) \dot{x} = 0 \tag{71}$$

From the first equation, one has that

$$\|x(t)\| = \|x(0)\| \tag{72}$$

for all $t > 0$. In other words, while the norm of the parameter error vector is monotonically decreasing, the norm of the parameter vector is constant. In particular, the norm of the state is bounded for all time by its initial value, regardless of the local instability around one half of the equilibrium surface. (72) along with (15) indicate that any decrease in the magnitude of the first two estimated parameters $\sqrt{x_{1,av}^2 + x_{2,av}^2}$ must result in an increase in the magnitude of the other two estimated parameters $\sqrt{x_{3,av}^2 + x_{4,av}^2}$, and vice versa. Note that if the two magnitudes

changed proportionally in the same direction, there would be no change in control parameter and no impact on the output error. The second equation in (71) yields a further constraint on the state vector but is not as easily integrated as the first one.

D. Simulation

In this section, we discuss an example that illustrates the properties of the averaged system. Consider the nominal parameter

$$x^* = \begin{pmatrix} 1.0 & 1.0 & 1.0 & 1.0 \end{pmatrix}^T, \tag{73}$$

with the initial vector $x(0) = \begin{pmatrix} 1.1 & -2.0 & -2.0 & 1.0 \end{pmatrix}^T$ and the gain $\epsilon = 2.0$. The eigenvalues of (48) are given in (61). $x(0)$ was chosen in the neighborhood of an unstable equilibrium point whose eigenvalues have relatively large imaginary part. The trajectories of the parameter estimates were projected into the $(x_{1,av}, x_{2,av})$ plane for visualization in the simulation result of Fig. 7.

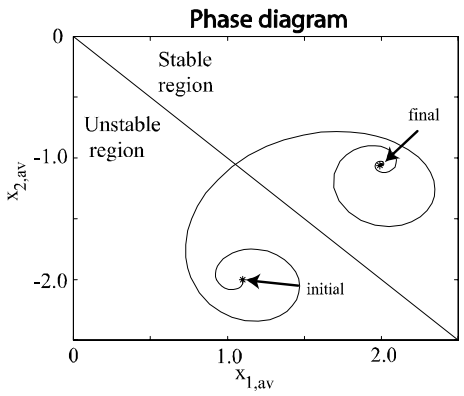

Fig. 7. Responses of identified parameters

With the initial conditions chosen close to the unstable region of the equilibrium surface, we see that the trajectory spirals with exponential growth as predicted, then crosses over into the stable region. The trajectory spirals back with exponential decay towards the equilibrium surface, as the eigenvalues turn out to also have large imaginary parts in that region. The unstable, highly oscillatory initial response was obtained by setting the initial estimate of the phase of the plant at

$$\measuredangle \hat{P}(j\omega_o) = -61.2^o. \tag{74}$$

while the phase of the plant was

$$\measuredangle P(j\omega_o) = 45^o \tag{75}$$

resulting in a phase difference of $\measuredangle P(j\omega_o) - \measuredangle \hat{P}(j\omega_o) = 106^o$ (beyond the 90^o angle condition, but close to it to ensure oscillatory behavior). The 90^o angle condition pertains to the mixed time scale system (26)-(27) when the

plant estimate is not updated online, such as the standard LMS algorithm. It states that for stability of the averaged system (30) it is both sufficient and necessary that $P_R\hat{P}_R+P_I\hat{P}_I > 0$, or equivalently $\left|\angle P(j\omega_o) - \angle\hat{P}(j\omega_o)\right| < 90^o$ [30, p.163]. Although not shown, it was verified that the norm of trajectories remained constant at $\|x(t)\| = \|x(0)\| = 3.20$.

V. Experiments

A. Results with the adaptive algorithm

The performance of the algorithm given by (11), (12), and (15) was examined through single-channel active noise control experiments. The active noise control system was the same system used to identify the 250 coefficient FIR transfer function used in section III.D. In the experiments of this subsection and of the subsection that follows, the parameters of the plant remain unchanged. The algorithm was coded in C and implemented via a dSpace DS1104 digital signal processing board. A sampling frequency of $8\ kHz$ was used. A constant amplitude sinusoidal disturbance with frequency of $185\ Hz$ was generated by one loudspeaker, while the control signal was produced by another. The phase of the plant was estimated experimentally at $93.2°$. The initial plant estimate was set at $P(j\omega) = \begin{pmatrix} -0.01 & 0.1 \end{pmatrix}^T$, corresponding to a phase angle of $95.7°$ and a phase difference of $2.5°$. Using these initial conditions along with an adaptation gain of 10 results in the parameter convergence seen in Fig. 8. The corresponding error attenuation is shown in Fig. 9. The parameters converge to values which give significant noise attenuation.

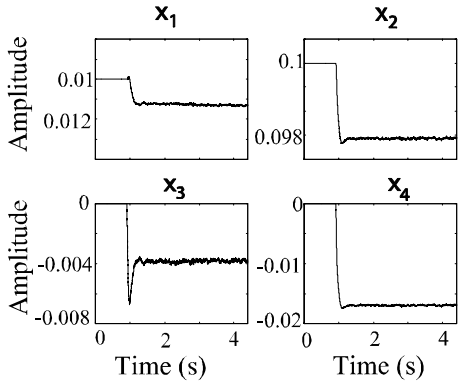

Fig. 8. Adaptive algorithm with small initial phase difference: parameter convergence.

Next, an initial plant estimate with $P(j\omega) = \begin{pmatrix} 0.1 & -0.01 \end{pmatrix}^T$ was used, corresponding to a phase angle of $-5.7°$ and a phase difference of $98.9°$, beyond the $90°$ phase condition. After some initial oscillations, the parameters are seen to converge in Fig. 10 . The corresponding error is shown in Fig. 11. Starting from the unstable region simply results in a slightly longer transient.

Although the initial conditions of the system produce a locally unstable adaptive system, the dynamics are such that convergence to a non-unique equilibrium state is eventually achieved. In the transient, the parameter error

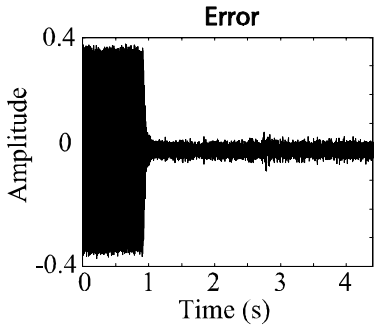

Fig. 9. Adaptive algorithm with small initial phase difference: error attenuation.

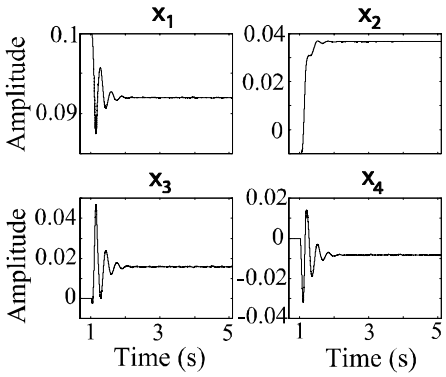

Fig. 10. Adaptive algorithm with large initial phase difference: parameter convergence.

vector and the parameter vector remain bounded by their initial value. In the steady-state, the parameter vector is such that the nominal control vector is reached.

B. Comparison to standard LMS algorithm

A standard algorithm in active noise and vibration control is the filtered-X LMS algorithm [26, p.62]. It is a gradient-type algorithm of which we present an implementation here for the sake of comparison. Recalling (6), the steady-state output of the plant is

$$y = w_1^T G^* \theta + p = w_1^T G^* \left(\theta - \theta^*\right) \tag{76}$$

The error y^2 can be minimized by using the gradient algorithm [2]

$$\dot{\theta} = -\epsilon G^{*T} w_1 y \tag{77}$$

The corresponding averaged system

$$\dot{\theta} = -\frac{\epsilon}{2} G^{*T} G^* \left(\theta - \theta^*\right) \tag{78}$$

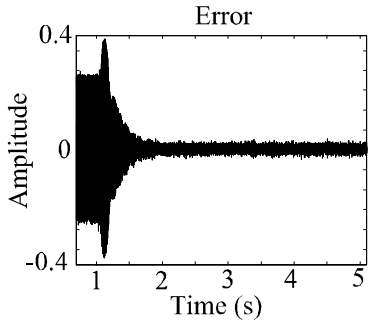

Fig. 11. Adaptive algorithm with large initial phase difference: error attenuation.

has a unique equilibrium at $\theta = \theta^*$ that is exponentially stable if $G^* \neq 0$. If G^* is not known, an a priori estimate G of G^* is used, and the averaged system becomes [2]

$$\dot{\theta} = -\frac{\epsilon}{2} G^T G^* \left(\theta - \theta^*\right) \tag{79}$$

$\theta = \theta^*$ is still an equilibrium, but it is unique and exponentially stable if and only if the eigenvalues of

$$G^T G^* = \begin{pmatrix} x_1 & -x_2 \\ x_2 & x_1 \end{pmatrix} \begin{pmatrix} x_1^* & x_2^* \\ -x_2^* & x_1^* \end{pmatrix} \tag{80}$$

lie in the open right half plane. The condition for stability is again that

$$x_1 x_1^* + x_2 x_2^* > 0 \tag{81}$$

which requires that the phase of the initial estimate of the plant be within 90° of the true value.

Experiments with the filtered-X LMS algorithm show the benefits of the algorithm of (11), (12), and (15). In the first experiment, the plant estimate $P(j\omega)$ has a phase difference of 1.7° with respect to the actual plant. Using the estimate along with an adaptation gain of 75, the responses of the parameters can be seen in Fig. 12, and the corresponding error attenuation can be seen in Fig. 13. As expected, the parameters converge to values that result in significant noise cancellation.

Next, a phase difference of 99.8° was applied In Fig. 14, the parameters are seen to experience divergence which results in the exponential growth of the error in Fig. 15. Comparing these results with those obtained in the previous section, one finds interesting similarities between the stability regions of the algorithms. With the algorithm of (11), (12), and (15), however, on-line identification produces a nonlinear system where trajectories eventually converge to the vicinity of a stable equilibrium, regardless of the initial error in the estimate of the phase of the true plant.

VI. Experiments with least-squares algorithm and time-varying systems

In the experiments of this subsection, the parameters of the plant are allowed to change significantly with time. In some situations, it may be desirable to use a least-squares algorithm for its superior convergence properties. A

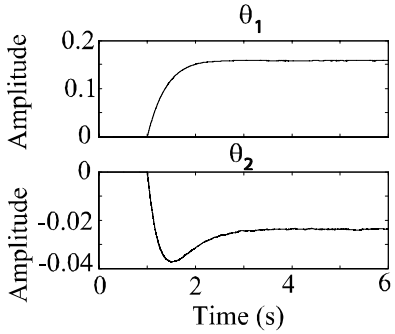

Fig. 12. LMS algorithm with small initial phase difference: parameter convergence.

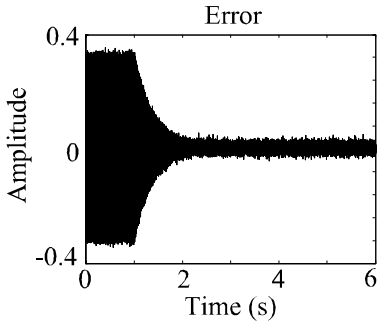

Fig. 13. LMS algorithm with small initial phase difference: error attenuation.

discrete-time implementation [18] is available that incorporates a stabilizing mechanism to insure stability while still allowing for rapid convergence. The parameter vector x is obtained by minimizing the cost function

$$E\left[x(n)\right] = \sum_{k=1}^{n} (e(k) - W^T(k)x(n))^2 \lambda^{n-k} + \alpha \left|x(n) - x(n-1)\right|^2 \tag{82}$$

where λ is a forgetting factor and α is a stabilizing factor. Note that this criterion incorporates a penalty on the parameter variation, while for $\alpha = 0$, the standard least-squares with forgetting factor is recovered. Setting $\partial E/\partial \hat{x}(n) = 0$, the estimate that minimizes (82) is

$$x(n) \quad = \quad \left(\sum_{k=1}^{n} W(k)W^T(k)\lambda^{n-k} + \alpha I_{4x4} \right)^{-1} \times \left(\sum_{k=1}^{n} W(k)e(k)\lambda^{n-k} + \alpha x(n-1) \right) \tag{83}$$

From this batch formula, an equivalent recursive formulation can be found as

$$K^{-1}(n) \quad = \quad \lambda K^{-1}(n-1) + W(n)W^T(n) + \alpha(1-\lambda)I_{4x4} \tag{84}$$

$$x(n) \quad = \quad x(n-1) + K(n)W(n)(e(n) - W^T(n)x(n-1)) + \alpha\lambda K(n)(x(n-1) - x(n-2)) \tag{85}$$

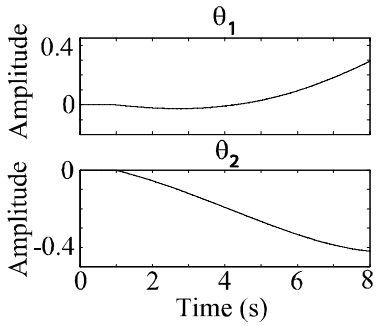

Fig. 14. LMS algorithm with large initial phase difference: parameter convergence.

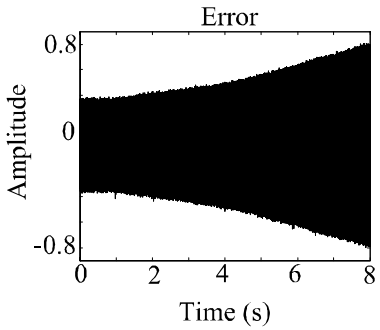

Fig. 15. LMS algorithm with large initial phase difference: error attenuation.

where

$$K^{-1}(0) = \alpha I_{4x4}. \tag{86}$$

A forgetting factor $\lambda < 1$ causes the influence of old data on the identification of x to be reduced as time proceeds, enabling the algorithm to track variations in the true parameters. From [18], the averaged system corresponding to (84)-(85) is given by

$$K_{av}^{-1}(n) = \lambda K_{av}^{-1}(n-1) + E(x)E^T(x) + \alpha(1-\lambda)I_{4x4} \tag{87}$$

$$\theta_{av}(n) = \theta_{av}(n-1) - K_{av}(n)E(x)E^T(x)\theta_{av}(n-1) + \alpha\lambda K_{av}(n)\left(\theta_{av}(n-1) - \theta_{av}(n-2)\right). \tag{88}$$

The least-squares algorithm was tested with challenging test conditions requiring continuous adaptation. A constant amplitude sinusoidal disturbance with frequency of $185\ Hz$ was assumed. Plant parameters were initialized at $x_1(0) = x_2(0) = 1.0$, and disturbance parameters were initialized at $\mathrm{x}_3(0) = x_4(0) = 0$. A forgetting factor $\lambda = 0.999$ was used. This choice corresponds to a time constant of $1,000$ samples, or 0.125 seconds. A value of $\alpha = 75$ was chosen. The covariance matrix was started at (86). (84) was used to update $K^{-1}(n)$ and the inverse was taken for use in updating x. These results were obtained using the control structure of Fig. 2.

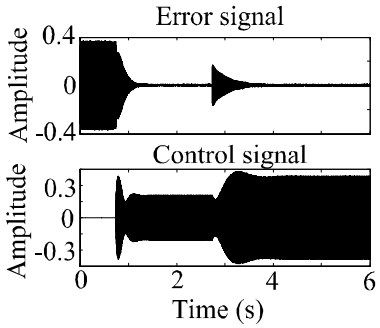

Fig. 16. Error and control signals with fixed true parameters and microphone switched at ≈ 2.75 s.

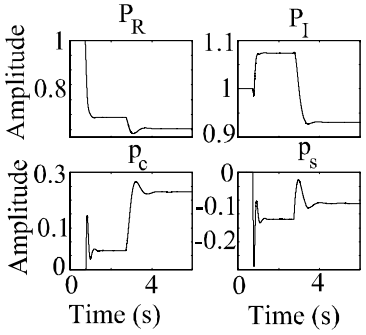

Fig. 17. Identified parameters when true parameters suddenly change.

An error microphone provided feedback to the algorithm, and attenuation results can be seen in Fig. 16. The estimated parameters can be seen in Fig. 17. The control algorithm was engaged after approximately $0.75s$ and convergence occurred in less than one half second. Unknown to the algorithm, the microphone used for cancellation was abruptly switched at approximately $2.75s$ to a microphone located some $4\ feet$ away. After a brief time interval, the algorithm was able to compensate for the change in plant parameters, again in less than half a second.

The ability to track slow time variations in system parameters was also explored. In Fig. 18 and Fig. 19, the result of manually moving the error sensor within the field of cancellation are shown. In these figures, the parameters were frozen after reaching the initial steady-state The error signal is shown along with the frozen control signal. Significant errors occur once the microphone has moved sufficiently to alter the characteristics of the system in a significant way.

In Fig. 20, the algorithm is allowed to track the time-varying parameters. Significant attenuation is now observed despite the fact that both plant and disturbance parameters are changing. The identified parameters are shown in Fig. 21.

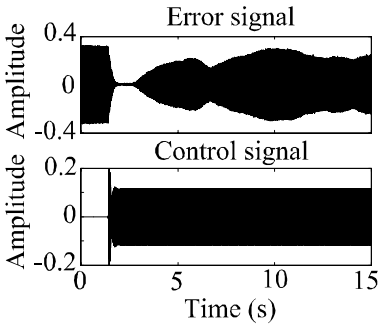

Fig. 18. Error and control signals with continuously changing parameters but frozen estimates.

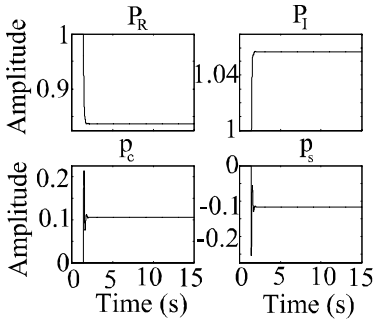

Fig. 19. Parameter estimates frozen after reaching steady-state.

VII. Extension of the algorithm

A. MIMO case

In the extension of the algorithm (11), (12), and (15), assume that there are i outputs of $P(s)$ and j inputs. Take the disturbance as consisting of a single sinusoidal component, and apply the algorithm of (11), (12), and (15) at each output. At each plant output, there are $2j$ plant parameters and 2 disturbance parameters to be identified, giving a regressor at each output of the form

$$W_i(t,\theta) = \begin{pmatrix} u_v \\ \tilde{u}_v \\ \cos(\omega_1 t) \\ \sin(\omega_1 t) \end{pmatrix} \tag{89}$$

where

$$u_v = \begin{pmatrix} u_1(t) \\ \vdots \\ u_j(t) \end{pmatrix}, \quad \tilde{u}_v = \begin{pmatrix} \tilde{u}_1(t) \\ \vdots \\ \tilde{u}_j(t) \end{pmatrix} \tag{90}$$

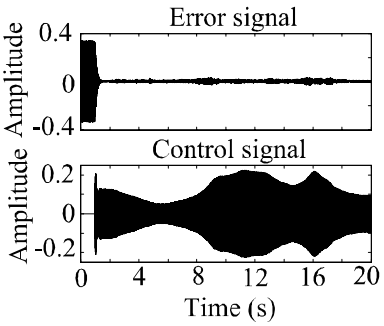

Fig. 20. Error and control signals with continuously changing system parameters.

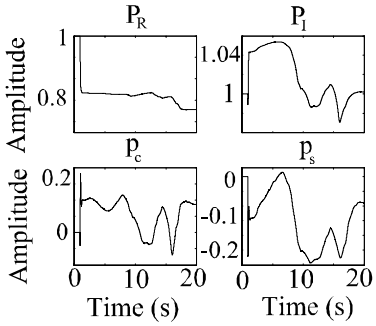

Fig. 21. Tracking of continuously changing parameters.

and each u_j, $\tilde{u}_j$ correspond to a plant input. This leads to a state vector of the form

$$x_i(t) = \begin{pmatrix} \hat{P}_{Ri1} & \cdots & \hat{P}_{Rij} & \hat{P}_{Ii1} & \cdots & \hat{P}_{Iij} & \hat{p}_{ci} & \hat{p}_{si} \end{pmatrix}^T \tag{91}$$

For clarity, the individual elements of the vector $x_i(t)$ are denoted by the estimate of the corresponding element of x_i^*. For calculation of the control coefficients, the states of each algorithm can be combined as

$$G = \begin{pmatrix} \hat{P}_R & \hat{P}_I \\ -\hat{P}_I & \hat{P}_R \end{pmatrix}, \pi = \begin{pmatrix} \hat{p}_c \\ \hat{p}_s \end{pmatrix} \tag{92}$$

where

$$\hat{P}_R = \begin{pmatrix} \hat{P}_{R11} & \cdots & \hat{P}_{R1j} \\ \vdots & \ddots & \vdots \\ \hat{P}_{Ri1} & \cdots & \hat{P}_{Rij} \end{pmatrix}, \hat{P}_I = \begin{pmatrix} \hat{P}_{I11} & \cdots & \hat{P}_{I1j} \\ \vdots & \ddots & \vdots \\ \hat{P}_{Ii1} & \cdots & \hat{P}_{Iij} \end{pmatrix} \tag{93}$$

and

$$\hat{p}_c = \begin{pmatrix} \hat{p}_{c1} \\ \vdots \\ \hat{p}_{ci} \end{pmatrix}, \quad \hat{p}_s = \begin{pmatrix} \hat{p}_{s1} \\ \vdots \\ \hat{p}_{si} \end{pmatrix} \tag{94}$$

The control coefficients are determined by

$$\theta = -G^{-1}\pi \tag{95}$$

where

$$\theta = \begin{pmatrix} \theta_{c1} & \cdots & \theta_{cj} & \theta_{s1} & \cdots & \theta_{sj} \end{pmatrix}^T \tag{96}$$

In (95), the appropriate pseudo-inverse should be used for cases where $i \neq j$. The initial conditions of each x_i must be chosen so that G is not singular, but all other initial conditions can be 0. The jth plant input is found as

$$u_j(t) = \theta_{cj}\cos(\omega_1 t) + \theta_{sj}\sin(\omega_1 t) \tag{97}$$

In order to demonstrate this extension of the algorithm, an active noise control experiment is presented. The plant consists of 2 inputs (control loudspeakers) and 2 outputs (error microphones). The disturbance is a $160\ Hz$ sinusoid. The initial conditions of each x_i were chosen as

$$x_1(0) = \begin{pmatrix} 1 & 1 & 0 & 0 & 0 & 0 \end{pmatrix}^T \tag{98}$$

$$x_2(0) = \begin{pmatrix} 0 & 0 & 1 & 1 & 0 & 0 \end{pmatrix}^T \tag{99}$$

The results of the experiment can be seen in Fig.22, where significant attenuation is observed at each output of the plant.

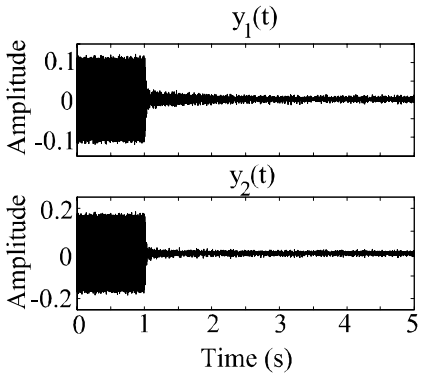

Fig. 22. Output error with 2 inputs and 2 outputs.

B. Multiple frequency components

The algorithm of (11), (12), and (15) can also be extended for the rejection of a periodic disturbance consisting of multiple sinusoidal components. A disturbance consisting of m sinusoidal components is written in the form of (2) as

$$p(t) = w_m^T \pi^* \tag{100}$$

where the vector

$$w_m(t) = \begin{pmatrix} v_{\cos} \\ v_{\sin} \end{pmatrix} \tag{101}$$

consists of

$$v_{\cos} = \begin{pmatrix} \cos(\omega_1 t) \\ \vdots \\ \cos(\omega_m t) \end{pmatrix}, v_{\sin} = \begin{pmatrix} \sin(\omega_1 t) \\ \vdots \\ \sin(\omega_m t) \end{pmatrix} \tag{102}$$

and the vector

$$\pi^* = \begin{pmatrix} p_c \\ p_s \end{pmatrix} \tag{103}$$

consists of

$$p_c = \begin{pmatrix} p_{c,1} \\ \vdots \\ p_{c,m} \end{pmatrix}, \quad p_s = \begin{pmatrix} p_{s,1} \\ \vdots \\ p_{s,m} \end{pmatrix} \tag{104}$$

Each ω_m, $p_{c,m}$, $p_{s,m}$ corresponds to a specific sinusoidal component of the disturbance. We have the regressor

$$W(t,\theta) = \begin{pmatrix} u_v \\ \tilde{u}_v \\ \cos(\omega t) \\ \sin(\omega t) \end{pmatrix} \tag{105}$$

where

$$u_v = \begin{pmatrix} u_{,1}(t) \\ \vdots \\ u_{,m}(t) \end{pmatrix}, \qquad \tilde{u}_v = \begin{pmatrix} \tilde{u}_{,1}(t) \\ \vdots \\ \tilde{u}_{,m}(t) \end{pmatrix} \tag{106}$$

and

$$u_{,m}(t) = \theta_{c,m} \cos(\omega_m t) + \theta_{s,m} \sin(\omega_m t) \tag{107}$$

$$\tilde{u}_{,m}(t) = \theta_{s,m} \cos(\omega_m t) - \theta_{c,m} \sin(\omega_m t) \tag{108}$$

These definitions lead to a vector of identified parameters of the form

$$x(t) = \begin{pmatrix} \hat{P}_{R,1} & \cdots & \hat{P}_{R,m} & \hat{P}_{I,1} & \cdots & \hat{P}_{I,m} & \hat{p}_c & \hat{p}_s \end{pmatrix}^T \tag{109}$$

where

$$\hat{p}_c = \begin{pmatrix} \hat{p}_{c,1} \\ \vdots \\ \hat{p}_{c,m} \end{pmatrix}, \quad \hat{p}_s = \begin{pmatrix} \hat{p}_{s,1} \\ \vdots \\ \hat{p}_{s,m} \end{pmatrix} \tag{110}$$

Again for clarity, the individual elements of the vector $x(t)$ are denoted by the estimate of the corresponding element of x^*.Calculation of the control coefficients can be combined as

$$G = \begin{pmatrix} \hat{P}_R & \hat{P}_I \\ -\hat{P}_I & \hat{P}_R \end{pmatrix}, \pi = \begin{pmatrix} \hat{p}_c \\ \hat{p}_s \end{pmatrix} \tag{111}$$

where

$$\hat{P}_R = \begin{pmatrix} \hat{P}_{R,1} & 0 & 0 \\ 0 & \ddots & 0 \\ 0 & 0 & \hat{P}_{R,m} \end{pmatrix}, \hat{P}_I = \begin{pmatrix} \hat{P}_{I,1} & 0 & 0 \\ 0 & \ddots & 0 \\ 0 & 0 & \hat{P}_{I,m} \end{pmatrix} \tag{112}$$

The control coefficients are found similar to (95) by

$$\theta = -G^{-1}\pi \tag{113}$$

but now

$$\theta = \begin{pmatrix} \theta_{c,1} & \cdots & \theta_{c,m} & \theta_{s,1} & \cdots & \theta_{s,m} \end{pmatrix}^T \tag{114}$$

The control signal is found as

$$u(t) = u_{,1}(t) + u_{,2}(t) + \cdots + u_{,m}(t) = w_m^T\theta \tag{115}$$

In order to demonstrate this extension of the algorithm, an active noise control experiment is presented. The plant consists of a single input (loudspeaker) and a single output (microphone). The disturbance consisted of two sinusoidal components of 180 Hz and 160 Hz respectively. The initial x was

$$x = \begin{pmatrix} -0.04 & -0.7 & 1.04 & 1.4 & 0 & 0 & 0 & 0 \end{pmatrix}^T \tag{116}$$

The result of the experiment can be seen in Fig. 23, where significant attenuation is observed.

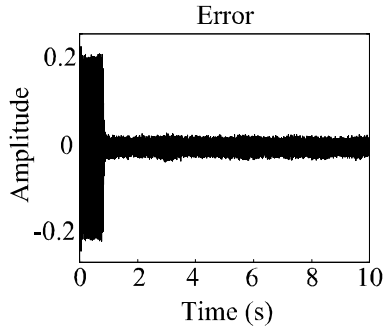

Fig. 23. Plant output with disturbance consisting of 2 frequency components.

VIII. Conclusions

An adaptive algorithm for the rejection of periodic disturbances of known frequency affecting unknown plants was considered. Typically, in active noise and vibration control applications, the plant is approximately linear, allowing a linear expression at the output of the plant to be derived. The unknown parameters were collected in a vector, and an estimate of this vector formed the states of a nonlinear controller. Since the overall closed-loop system was nonlinear and time-varying, averaging theory was applied to analyze the system. By averaging over time, a much simpler time-invariant system was obtained, whose dynamics closely approximated the dynamics of the actual system. It was shown that the averaged system for the algorithm under consideration was a 4-dimensional nonlinear system with a 2-dimensional equilibrium surface. Half of the surface was locally stable and the other half was unstable. Generally, trajectories converged to the stable subset of the equilibrium surface, resulting in cancellation of the disturbance. Further properties of the trajectories of the systems were obtained from an analysis of the averaged system Simulations and single-channel active noise control experiments illustrated the results. It was found that stability was achieved in situations that would be unstable with simpler algorithms that do not provide plant adaptation. In addition, the ability to track abruptly or continuously time-changing system parameters was demonstrated. While we have considered disturbances of known frequency, many real-world scenarios contain unknown frequencies that may drift over time. As such, future work will combine the adaptive algorithm presented here with frequency estimation techniques [34] in order to reject disturbances of unknown and time-varying frequency acting on unknown and time-varying systems.

IX. Appendix

A. Verification of assumptions B1-B6

The original and averaged systems are given by

$$f(t,x,x_P) = -E(x)w_1(t)\left(w_1^T(t)E^T(x)x - Cx_P - w_1^T(t)\pi^*\right) \tag{117}$$

$$f_{av}(x) = -\frac{1}{2}E(x)E^T(x)(x-x^*) \tag{118}$$

and

$$d(t,x) = f(t,x,v(t,x)) - f_{av}(x) \tag{119}$$

$$= -E(x)\left(w_1(t)w_1^T(t) - \frac{1}{2}I_{2\times 2}\right)E^T(x)(x-x^*) + E(x)w_1(t)y_{tr}(t) \tag{120}$$

where $y_{tr}(t)$ decays exponentially to zero. In the verification of B1-B6, assumption B7 will be assumed to hold. Then, we have the following:

For some arbitrary vector $x \in R^n$ and for some $h > 0$ such that $B_h = \{x \in \mathbb{R}^n \,|\|x\| < h\}$

B1 Due to the sinusoidal variation of w_1, f is continuous in t. Due to assumption B7 and the BIBO stability of $P(s)$, f is a smooth continuous function in x, x_P for all $t \geq 0$ and $x, x_P \in B_h$. Again, as a result of B7, $\{\partial f/\partial[x, x_P]\}$ is bounded for all $t \geq 0$ and $x, x_P \in B_h$.

B2 In the main text it is shown that the averaged system (118) can be obtained from the original system (117) and, due to assumption B7, $\partial f_{av}/\partial x$ is continuous and bounded for all $x \in B_h$.

B3 Since averaging is done with respect to time, $d(t,x)$ and $\frac{\partial d(t,x)}{\partial x}$ have zero average value. Further, the following bounds can be derived

$$\begin{aligned}\left|\frac{1}{T}\int_{t_0}^{t_0+T} d(\tau,x)d\tau\right| &\leq \frac{1}{T}\gamma_1(T)\left\|x\right\| + \tilde{\gamma}(T)\\ \left|\frac{1}{T}\int_{t_0}^{t_0+T} \frac{\partial d(t,x)}{\partial x}d\tau\right| &\leq \frac{1}{T}\gamma_2(T)h\end{aligned}$$

where

$$\gamma_1(T) = \frac{1}{2\omega\left\|\hat{P}(j\omega)\right\|^2}\left[\left\|\hat{P}(j\omega)\right\|^2\left\|\pi\right\|^2 + \left\|\hat{\pi}\right\|^2\left\|P(j\omega)\right\|^2 - 2\left\|P(j\omega)\right\|^2\left\|\hat{P}(j\omega)\right\|^2(\theta_c\theta_c^* + \theta_s\theta_s^*)\right]^{\frac{1}{2}},$$

$$\gamma_2(T) = \frac{1}{2\omega\left\|\hat{P}(j\omega)\right\|^2}\left[\left\|x^*\right\|^2 + 4\left\|P(j\omega)\right\|^2\left(\frac{\left\|\hat{\pi}\right\|^2}{\left\|\hat{P}(j\omega)\right\|^2} - \theta_c\theta_c^* - \theta_s\theta_s^*\right)\right]^{\frac{1}{2}},$$

and $\tilde{\gamma}(T)$ converges exponentially to 0 with y_{tr} for all $x \in B_h$. Then, one can write

$$\gamma(T) = \frac{1}{T}\max[\gamma_1(T), \gamma_2(T)h]$$

for all $x \in B_h$. Further, by assumption B7 and due to the sinusoidal variation of w_1, $d(t,x)$ has a bounded integral with respect to time for all $t \geq 0$ and $x \in B_h$.

B4 This assumption can be verified for the vast majority of active noise and vibration control applications for which this algorithm is designed.

B5 This assumption follows directly from the constraint on the averaged system (72) derived in the main text and the bounded-input bounded-output (BIBO) stability of $P(s)$.

B6 This assumption is satisfied as a consequence of the BIBO stability of $P(s)$.

B7 This assumption is satisfied as long as the magnitude of the plant frequency response does not approach zero. While the amplitude response in active noise and vibration control applications may exhibit dramatic dips due to the interaction of signal reflections, this can be avoided by appropriate arrangement of the hardware.

X. References

References

[1] A. Sacks, M. Bodson, & P. Khosla, "Experimental Results of Adaptive Periodic Disturbance Cancellation in a High Performance Magnetic Disk Drive," *ASME Journal of Dynamics Systems, Measurement, and Control*, vol. 118, pp. 416-424, 1996.

[2] B. Wu & M. Bodson, "Multi-Channel Active Noise Control for Periodic Sources – Indirect Approach," Automatica, vol 40, no. 2, pp. 203-212, 2004.

[3] B. D. O. Anderson, R. R. Bitmead, C. R. Johnson, P. V. Kokotovic, R. L. Kosut, I. M. Y. Mareels, L. Praly, & B.D. Riedle, *Stability of Adaptive Systems. Passivity and Averaging Analysis*. MIT Press, Cambridge, MA 1986.

[4] C. R. Knospe, S. J. Fedigan, R. W. Hope, & R. D. Williams, “A Multi-Tasking Implementation of Adaptive Magnetic Bearing Control,” *IEEE Trans. on Control Systems Technology*, vol. 5, no. 2, pp. 230-238, 1997.

[5] D. Patt, J. Chandrasekar, D. S. Bernstein, & P.P. Friedmann, “Higher-Harmonic-Control Algorithm for Helicopter Vibration Reduction Revisited,” *AIAA Journal of Guidance, Control, and Dynamics*, vol. 28, no. 5, pp. 918-930, 2005.

[6] D. R. Morgan, “An Analysis of Multiple Correlation Cancellation Loops with a Filter in the Auxiliary Path,” *IEEE Trans. on Speech and Signal Processing*, vol. 28, no. 4, pp. 454-467, 1980.

[7] E. Kamen and B. Heck, *Fundamentals of Signals and Systems: Using the Web and Matlab, 2nd Edition*, New Jersey, Prentice Hall, 2000.

[8] G. Feng & M. Palaniswamy,“Adaptive Implementation of Internal Model Principle for Continuous Time Systems,” *IEE Proceedings-D*, vol. 139, no. 2, pp. 167-171, 1992.

[9] G. Feng & M. Palaniswamy, “A Stable Adaptive Implementation of the Internal Model Principle,” *IEEE Trans. on Automatic Control*, vol. 37, no. 8, pp. 1220-1225, 1992.

[10] G. Tao, *Adaptive Control Design and Analysis*, Wiley, Hoboken, New Jersey, 2003.

[11] H. G .M. Dötsch, H. T. Smakman, P. M. J. Van den Hof, & M. Steinbuch, “Adaptive Repetitive Control of a Compact Disc Mechanism,” *Proc. of the Conference on Decision and Control*, New Orleans, LA, pp. 1720-1725, 1995.

[12] H.K. Khalil, *Nonlinear Systems,* 3rd ed., Prentice Hall, New Jersey, 2002.

[13] J. Chanderasekar, L. Liu, D. Patt, P. P. Friedmann, & D. S. Bernstein, ”Adaptive Harmonic Steady-State Control for Disturbance Rejection”, *IEEE Trans. on Control Systems Technology*, vol. 14, no. 6, pp. 993-1007, 2006.

[14] J. Lau, S. S. Joshi, B. N. Agrawal, & J.-W. Kim, “Investigation of Periodic-Disturbance Identification and Rejection in Spacecraft,” *AIAA Journal of Guidance, Control, and Dynamics*, vol. 29, no. 4, pp. 792-798, 2006.

[15] J. Spanos, Z. Rahman and G. Blackwood, “A Soft 6-Axis Active Vibration Isolator,” *Proc. American Control Conference,* Seattle, WA, pp. 412-416, 1995.

[16] K.S. Narendra & A. Annaswamy, *Stable Adaptive Systems*, Prentice-Hall, Englewood Cliffs, NJ, 1989.

[17] M. A. McEver, D. G. Cole, & R. L. Clark, “Adaptive Feedback Control of Optical Jitter Using Q-parameterization,” *Opt. Eng.*, vol. 43, no. 4, pp. 904-910, 2004.

[18] M. Bodson, “An Adaptive Algorithm with Information-Dependent Data Forgetting,” *Proc. of the American Control Conference*, Seattle, WA, pp. 3485-3489, 1995.

[19] M. Bodson, “Rejection of Periodic Disturbances of Unknown and Time-Varying Frequency,” *International Journal of Adaptive Control and Signal Processing*, vol. 19, pp. 67-88, 2005.

[20] M. Steinbuch, “Repetitive control for systems with uncertain period-time,” *Automatica*, vol. 38, no. 12, pp. 2103-2109, 2002.

[21] M. Zhang, H. Lan, & W. Ser, ”An Improved Secondary Path Modeling Method for Active Noise Control Systems,” *IEEE Signal Processing Letters*, vol. 7, no. 4, pp. 73-75, 2000.

[22] M. Zhang, H. Lan, & W. Ser, ”Cross-updated Active Noise Control System with Online Secondary Path Modeling,” *IEEE Trans. on Speech & Audio Processing*, vol. 9, no. 5, pp. 598-602, 2001.

[23] P. Ioannou & J. Sun, *Robust Adaptive Control*, Prentice-Hall, Upper Saddle River, New Jersey, 1996.

[24] S. Bittanti & L. Moiraghi, “Active Control of Vibrations in Helicopters via Pole Assignment Techniques,” *IEEE Trans. on Control Systems Technology,* vol. 2, no. 4, pp. 343-350, 1994.

[25] S.-C. Wu & M. Tomizuka, “Repeatable Runout Compensation for Hard Disk Drives Using Adaptive Feedforward Cancellation,” *Proc. of the American Control Conference*, Minneapolis, MN, pp. 382-387, 2006.

[26] S. M. Kuo & D. R. Morgan, *Active Noise Control Systems: Algorithms and DSP Implementations*, New York, Wiley, 1996.

[27] S. M. Kuo & D. Vijayan, ”A Secondary Path Modeling Technique for Active Noise Control Systems,” *IEEE Trans. on Speech and Audio Processing*, vol. 5, no. 4, pp. 374-377, 1997.

[28] S. Pigg & M. Bodson, “Adaptive Rejection of Sinusoidal Disturbances of Known Frequency Acting on Unknown Systems,” *Proc. of the American Control Conference*, Minneapolis, MN, pp. 4777-4781, 2006.

[29] S. Pigg & M. Bodson, “Rejection of Periodic Disturbances with Adaptation to Unknown Systems,” *Proc. of the European Control Conference*, Kos, Greece, pp. 2477-2483, 2007.

[30] S. Sastry and M. Bodson, *Adaptive Control: Stability, Convergence, and Robustness*, New Jersey, Prentice Hall, Englewood Cliffs, 1989.

[31] T. J. Manayathara, T.-C. Tsao, J. Bentsman, & D. Ross, “Rejection of Unknown Periodic Load Disturbances in Continuous Steel Casting Process Using Learning Repetitive Control Approach, *IEEE Trans. on Control Systems Technology*, vol. 4, no. 3, pp. 259-265, 1996.

[32] T. Meurers, S.M. Veres, & A.C.H. Tan, ”Model-free frequency domain iterative active sound and vibration control,” *Control Engineering Practice*, vol. 11, pp. 1049-1059, 2003.

[33] U. Emborg, “Cabin Noise Control in the Saab 2000 High-speed Turboprop Aircraft,” *Proc. of the ISMA 2*3, Brussels, Belgium, pp. 13-25, 1998.

[34] X. Guo & M. Bodson, “Frequency Estimation and Tracking of Multiple Sinusoidal Components,” *Proc. of the Conference on Decision and Control*, Maui, HI, pp. 5360-5365, 2003.

[35] X. Guo & M. Bodson, ”Analysis and Implementation of an Adaptive Algorithm for the Rejection of Multiple Sinusoidal Disturbances,” submitted to *IEEE Trans. on Control Systems Technology*, 2006.

[36] Y. H. Guan, W. S. Shepard Jr., T. C. Lim, & M. Li, “Experimental Analysis of an Active Vibration Control System for Gearboxes,” *Smart Mater. Struct.*, vol. 13, pp. 1230-1237, 2004.

[37] Y. Xu, M. de Mathelin, & D. Knittel, “Adaptive Rejection of Quasi-Periodic Tension Disturbances in the Unwinding of a Non-Circular Roll,” *Proc. of the American Control Conference*, Anchorage, AK, pp. 4009-4014, 2002.

[38] Y. Zhang, P. G. Mehta, R. R. Bitmead, & C. R. Johnson, ”Direct Adaptive Control for Tonal Disturbance Rejection,” *Proc. of the American Control Conference*, Philadelphia, PA, pp. 1480-1482, 1998.